NANO LETTERS

2007
Vol. 7, No. 9
2907−2912

Hyperbranched PbS and PbSe Nanowires and the Effect of Hydrogen Gas on Their Synthesis

Matthew J. Bierman, Y. K. Albert Lau, and Song Jin*

Department of Chemistry, University of Wisconsin—Madison, 1101 University Avenue, Madison, Wisconsin 53706

Received June 12, 2007; Revised Manuscript Received July 23, 2007

ABSTRACT

We report a chemical vapor deposition (CVD) synthesis of hyperbranched single-crystal nanowires of both PbS and PbSe using $PbCl_2$ and S/Se as precursors under hydrogen flow. Multiple generations of nanowires grow perpendicularly from the previous generation of nanowires in an epitaxial fashion to produce dense clusters of a complex nanowire network structure. The flow rate and duration of the hydrogen co-flow in the argon carrier gas during the CVD reactions are found to have a significant effect on the morphology of the PbS/PbSe grown, from hyperbranched nanowires to micrometer-sized cubes. No intentional catalyst was employed for the nanowire synthesis, but it is suggested that elemental lead that has been reduced from the vapor by the hydrogen might serve as a vapor–liquid–solid (VLS) catalyst for the anisotropic growth of PbS/PbSe. The nanowires were also investigated with Raman spectroscopy. These PbS and PbSe nanostructures can have applications in photovoltaics because multiple exciton generation has been demonstrated in nanocrystals of both materials.

Nanocrystals of lead selenide (PbSe) and lead sulfide (PbS) have been recently observed to exhibit multiple exciton generation in which up to seven excitons can be generated with a single incident high-energy photon in these narrow band gap (about 0.4 eV) materials.[1−3] This discovery has significant implications for high-efficiency photovoltaic energy generation because this can go beyond the fundamental Shockley−Queisser limit[4] ($\eta = 44\%$) for single-junction silicon photovoltaics and can approach an 800% quantum efficiency limit ($\eta = 65\%$) imposed by the 8-fold degeneracy of the band structure of these materials. The limitation of multiple exciton generation is short charge carrier lifetimes:[3] these carriers recombine through Auger recombination with lifetimes of a few hundred picoseconds, which prevents the photocarriers from being efficiently collected from a nanocrystal, resulting in reduced observed efficiencies.[5] One-dimensional nanowires,[6] hyperbranched nanowires,[7−9] nanowire heterostructures,[10−13] and other complex nanowire structures possess some advantages in the collection of photogenerated carriers over isolated nanocrystals. While still confined in two dimensions, photocarriers can be collected along the axial direction of the wire. Thus nanowires, particularly complex hyperbranched nanowires, of multiexciton generating materials such as PbS and PbSe would provide a direct electrical connection for carrier collection, which is potentially of great significance in solar energy harvesting.

Another reason for investigating the lead chalcogenide nanowire materials comes from the fact that they are isostructural (rock salt) and lattice-matched with the corresponding magnetic semiconducting europium chalcogenides (EuQ, Q = S, Se, Te).[14] Pb^{2+} has nearly identical ionic radius to Eu^{2+} and solid-state solutions exist for the entire composition range, for example, as shown in $Pb_{1-x}Eu_xTe$.[15] Ready incorporation of EuS (or EuSe) into thin films of PbS (or PbSe) have previously been shown to change the magnetic properties due to the magnetic Eu^{2+} ions and tune the band gap in the infrared range due to the wider bandgaps of EuQ.[16,17] Nanowires of alloyed $Pb_{1-x}Eu_xQ$ or epitaxial nanowire heterostructures between PbQ and EuQ will be interesting for the developing field of nanospintronics using magnetic semiconducting nanowires[18−21] and for IR detector materials.

Synthesis of PbS and PbSe nanocrystals has been investigated extensively,[1,22,23] but nanowires of PbS and PbSe have only recently began to emerge. Recent reports include the solution synthesis of straight PbS nanowires[24] and straight and branched PbSe nanowires,[23,25] as well as the hydrogen-free chemical vapor deposition (CVD) synthesis of PbS[26,27] and, very recently, hyperbranched PbSe nanowires.[28] Some synthesis[24,25,28] involved the addition of an intentional catalyst. In this letter, we report the synthesis and characterization of hyperbranched nanowires of both PbS and PbSe using a CVD method. Multiple levels of nanowires nucleate perpendicularly from the previous generation of nanowires

* Corresponding author. E-mail: jin@chem.wisc.edu.

10.1021/nl071405l CCC: $37.00
Published on Web 08/02/2007

in an epitaxial fashion to produce sometimes very dense clusters of complex nanowire network structures. Different from previous branched nanowire synthesis,[28] the PbS and PbSe nanowires were synthesized without the use of an intentional metal catalyst but with purposefully controlled hydrogen/carrier gas co-flow. The *crucial* role of hydrogen in the nanowire growth is systematically investigated, and the nanowires were examined with Raman spectroscopy.

The PbS/PbSe hyperbranched nanowires were synthesized in a home-built CVD reactor comprised of a 1 in. fused silica tube placed in a single-zone tube furnace (Lindberg\Blue M).[29] The sealed tube is equipped with pressure and multiple-gas flow control and a dry ice/acetone trap downstream before the vacuum pump. In an optimized reaction to form hyperbranched PbS nanowires, 30 mg of $PbCl_2$ (Sigma-Aldrich, 99.999%) in an alumina boat was placed inside the quartz tube at the center of the furnace, and a second alumina boat containing 60 mg of sulfur (Sigma-Aldrich, 99.5+%) was placed upstream just outside the mouth of the furnace ceramic insulation. A 3−5 mm wide strip of Si (100) substrate covered with 100 nm thermal SiO_2 was oxygen plasma cleaned and placed 1 cm downstream from the $PbCl_2$ boat. The quartz tube was evacuated and flushed 3 times with argon and then heated to 650 °C (the temperature at the center of the furnace where $PbCl_2$ is located) under 150 sccm of Ar and a pressure of 900 Torr. Once the target temperature was reached, the sulfur boat was inserted just inside the mouth of the furnace and 1 sccm of H_2 was co-flowed for 1 min, after which all hydrogen was shut off by closing both the flow meter and a secondary control valve. Reactions were terminated after 20 min by switching off the carrier gas and furnace, evacuating the tube and allowing the furnace to cool down with the lid opened. The $PbCl_2$ precursor in the boat was usually consumed at 10 min, while some sulfur powder remained after 20 min.

The resulting deposition was visible to unaided eyes as a "dust" on the otherwise mirrorlike substrate surface and on the wall of the silica tube nearby the substrate. Field emission scanning electron microscopy (SEM, LEO SUPRA 1530) revealed many clusters of nanowires on the substrate surface with little other deposition (Figure 1a). These clusters are about 30−60 μm large and contain often complex networks of many hyperbranched nanowires, as shown in the higher magnification images of a representative cluster (Figure 1b,c). Nanowires have a range of diameters for successive generations, with the final generation of nanowires having diameters of 75−125 nm. They grow 90° from each other, creating dense, intricate patterns due to branching (Figure 1b,c). Some experiments occasionally yielded branching nanostructures that are not as "developed" or crowded (Figure 1d), for which the multiple generations of branches and the orthogonal relationship between adjacent generations are more apparent. Transmission electron microscopy (TEM) analysis was carried out on nanowire samples ultrasonically removed from substrates into ethanol and dispersed on lacey carbon TEM grids using a Philips CM200 TEM. Low-magnification TEM (Figure 1e) further confirms the 90° relation between branches and trunk and reveals a slight diameter reduction

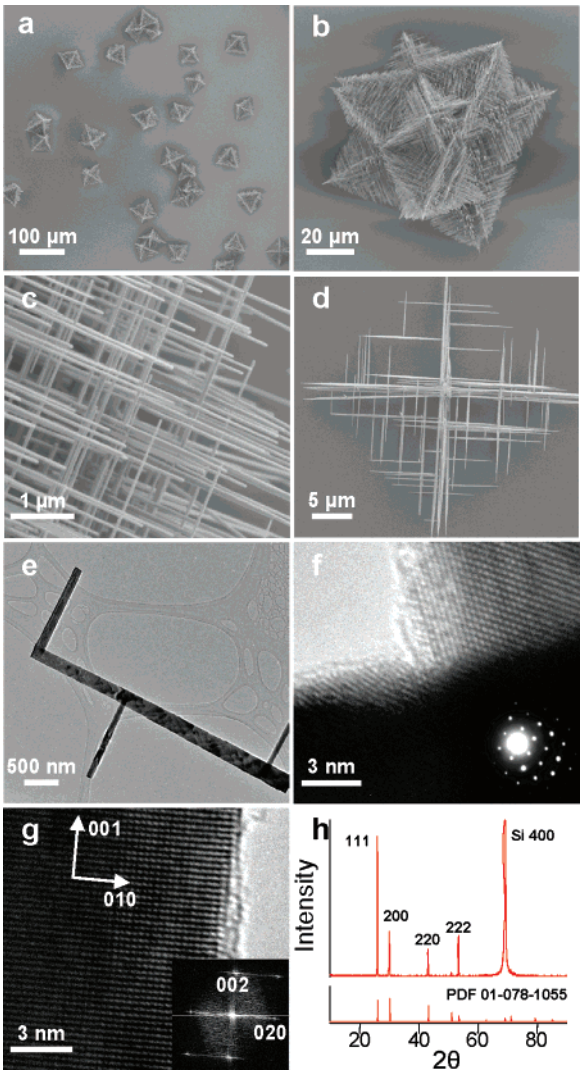

Figure 1. Hyperbranched PbS nanowires and their structural characterization. SEM micrographs show clusters of hyperbranched nanowire networks on substrate surface (a) from a dense, orthogonal network (b,c). Central stem nucleates and grows branches at 90°, as shown in SEM micrographs (d) and LRTEM images (e). (f) HRTEM and SAED (inset) along the [110] zone axis show the branches to be epitaxial. (g) Lattice-resolved HRTEM and corresponding indexed FFT (inset) show single-crystal PbS growing along the [001] axis. (h) PXRD that matches the PbS reference pattern.

in successive NW generations. No apparent metal catalyst balls were observed at the end of the nanowires in either TEM or SEM examination. HRTEM imaging and selected-area electron diffraction (SAED) of the branching points (Figure 1f) along the [110] zone axis show that the lattice planes are continuous from the trunk to the branch and they are epitaxial to each other. To positively identify the material, both HRTEM (Figure 1g) and powder X-ray diffraction (PXRD) were employed. EDS analysis on PbS is not fruitful because the commonly observed sulfur K line (2.47 keV) overlaps with the lead M_5 absorption edge (2.48 keV). Lattice-resolved HRTEM of one nanowire along the [100] zone axis (Figure 1g) shows lattice fringes and indexed FFT (inset of Figure 1g), consistent with the rock salt structure of PbS. The lattice parameter was calculated to be about

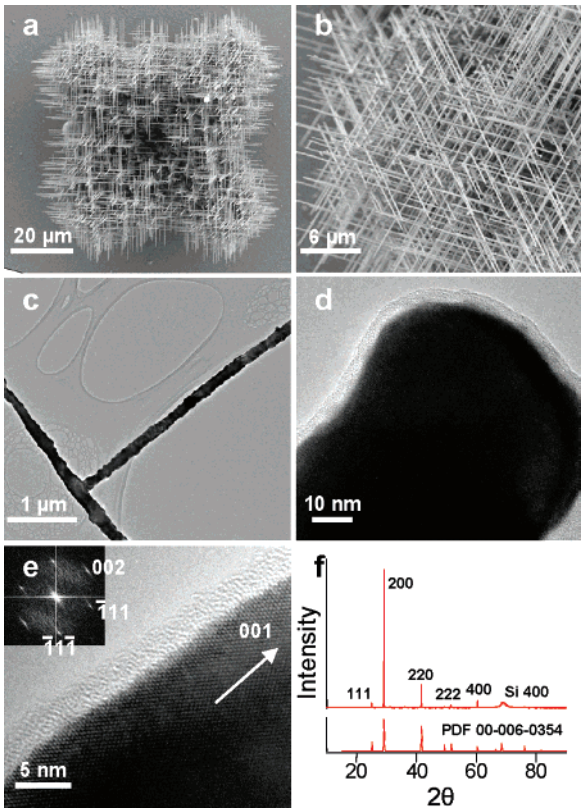

Figure 2. Hyperbranched PbSe nanowires and their structural characterization. SEM micrographs (a,b) show clusters of dense, orthogonally branched PbSe nanowires. LRTEM shows nanowire branching (c) as well as a lack of catalyst at the tip of nanowire branches (d). (e) HRTEM along the [110] zone axis shows a [001] growth direction for the nanowires. The indexed FFT is shown as inset. (f) PXRD further identifies the material as PbSe.

5.97 Å by using the lattice-resolved images or the FFT, which matches the 5.9362 Å of PbS reasonably well. The growth axis for all nanowires observed is along the ⟨001⟩ directions, which is consistent with the persistent 90° angle between trunk and branch. PXRD of as-grown nanowires on silicon substrates (Figure 1h) also confirms the material to be PbS, matching JCPDS PDF file 01-078-1055.

Lead selenide hyperbranched nanowires were also synthesized by using conditions analogous to those for PbS nanowires. For a typical synthesis, 100 mg of $PbCl_2$ and 175 mg of Se were employed. More importantly, optimal hyperbranched nanowire formation was found by using a bolus 20 sccm flow of the hydrogen for the initial 1 min of reaction then no additional hydrogen. Otherwise, the setup and conditions are identical to those for PbS nanowires. Under these optimized conditions, many nanowire clusters can be produced with relatively few other structures. Nanowires grow in hyperbranched clusters similarly to PbS (Figure 2a,b), showing 90° branching. The diameters of the narrowest nanowires are <100 nm, but most vary between 100 and 200 nm. EDS analysis (see Figure S1 in Supporting Information) performed in the TEM reveals Pb:Se in the ratio of 48:51, indicating PbSe within the error of the EDS analysis. HRTEM (Figure 2e) along the [110] zone axis shows the nanowire to be single crystalline and also have a [001] growth axis. Lattice parameters calculated from the FFT (6.15 Å) match the reported value (6.1243 Å), and the PXRD pattern in Figure 2f matches the reference PDF 00-006-0354. Similarly to PbS, no catalyst tips can be seen on any of the nanowires (Figure 2b,d). The PbSe nanowires are coated with a thin amorphous layer, which appears to contain Si by EDS analysis (see Figure S1 in Supporting Information). Previous reports have assigned such an amorphous layer as SiO_x.[26,27] Even though PbSe nanowires are always single crystalline, all SEM and TEM show the PbSe nanowires to have rougher surfaces than that of PbS nanowires. It is likely that higher hydrogen concentrations employed during the PbSe nanowire synthesis leads to more HCl production and more severe etching of the nanowires.

The key to reproducibly synthesize high-quality hyperbranched PbS and PbSe nanowires in large quantity is to control the hydrogen gas co-flow in the CVD growth process. It was previously reported that PbS nanowires were synthesized via CVD using $PbCl_2$ and S without hydrogen.[26] However, such reactions are somewhat inconsistent in our hands, and in the case when nanowires were produced, the yield was low and no hyperbranched nanowires were observed. Because hydrogen not only enhances the yield of the PbS/PbSe nanowire but also is crucial to the hyperbranched morphology, we have systematically investigated the influence of hydrogen by keeping all other experimental conditions as consistent as possible but varying the flow rate and duration of the hydrogen co-flow in the carrier gas. The particular case for PbSe is summarized in Figure 3, which shows representative SEM images illustrating the PbSe morphology dependence on the conditions of H_2 flow.

Two effects were investigated: the effect of a constant, low flow rate for varying duration and the effect of varying H_2 flow rate introduced during the initial growth stage. Panels a−d of Figure 3 show the effect of increasing hydrogen flow duration at a constant low flow rate of 1 sccm. When 1 sccm of H_2 co-flow is added for 1 min (Figure 3a), only minimal deposition is seen and consists primarily of nanowire nucleation centers—the primordial part of the dense, hyperbranched nanowire cluster (inset of Figure 3a). Prolonging this H_2 co-flow to 5 and 10 min (Figure 3b,c) show increasing density of deposition as well as a change in morphology to mostly micrometer-sized cubes. This is most predominant in Figure 3d, where 1 sccm of H_2 has been co-flown for the entire 20 min reaction. There is much deposition of large 5−10 μm cubes on the surface.

Panels a, e, f, and g of Figure 3 show the effect of increasing H_2 flow rates during the first minute of reaction. Again, starting with 1 sccm in Figure 3a, we mostly see the beginnings of nanowire nucleation sites on the surface. As the flow rate is increased to 10 sccm H_2 for 1 min (Figure 3e), the nanowire nucleation rate is higher and reasonably long nanowires (~10 μm) and somewhat developed nanowire clusters are deposited together with micrometer-sized particles. This trend continues through an optimum of 20 sccm H_2 for 1 min (Figure 3f), where even larger and full-fledged hyperbranched nanowire clusters are produced in high density. These are the conditions for the reported PbSe nanowires shown in Figure 2. However, if the flow

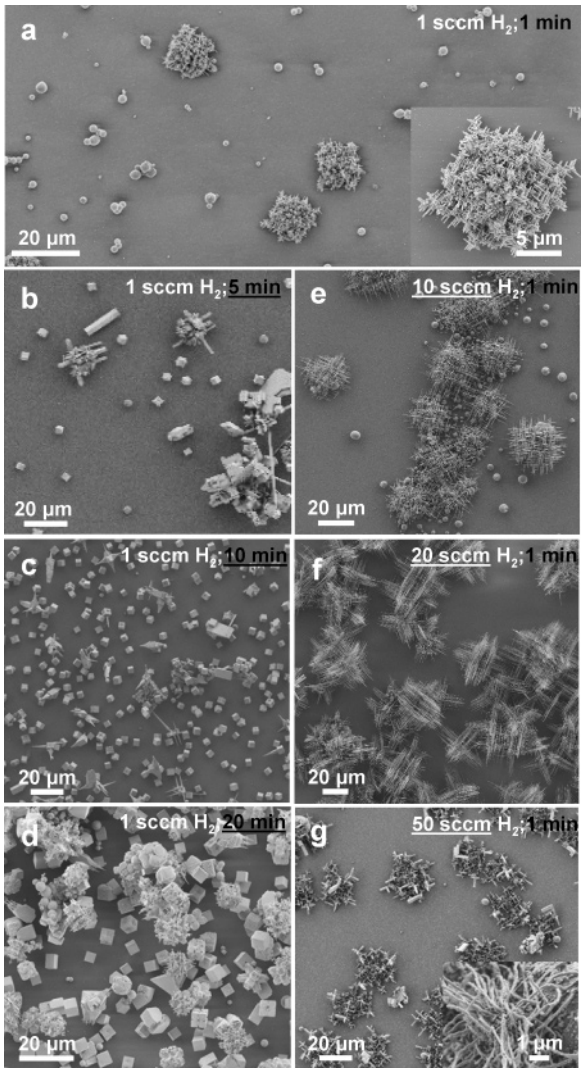

Figure 3. Effect of H_2 flow on PbSe nanowire nucleation and growth. Flow rates and times are indicated in the upper right of each panel. Insets in (a,g) are higher magnification SEM images highlighting the morphology of individual clusters.

rate is further increased to 50 sccm H_2 for 1 min (Figure 3g) the "nanowires" that form are no longer straight nor hyperbranched, as shown in the Figure 3g inset. There are many other regular or irregular structures deposited as well.

Overall, we have found that hydrogen must be present during the initial stages of CVD deposition to ensure the formation of nanowire morphology and that the more overall hydrogen present, especially late in the growth, tends to result in the deposition of cubes. A burst of H_2 feed for a short amount of time at the beginning is most conducive to producing the best (longest and most hyperbranched) nanowires. The case for PbS nanowires is qualitatively similar, but the amount of hydrogen flow for optimal growth of hyperbranched PbS nanowires (1 sccm for 1 min as reported above) is less than that for PbSe nanowires, perhaps due to the chemical differences between PbS and PbSe. In fact, the natural leak rate of the flow control meter was even sufficient to enable high-yield synthesis of PbS nanowires, which led to the original discovery of the crucial role of hydrogen.

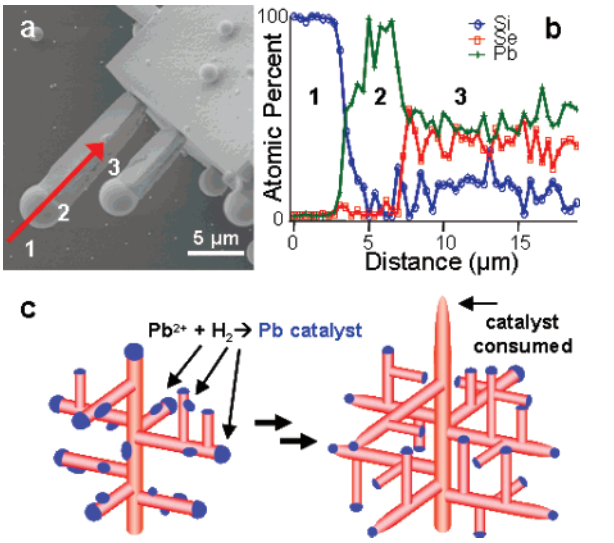

Figure 4. Role of Pb in the growth of PbS/PbSe wires. An SEM micrograph showing PbSe microrods (a) and EDS linescans (b) along the rod showing Pb caps on PbSe rods. (c) Proposed schematic mechanism for hyperbranched PbQ nanowire growth under the influence of H_2.

Unlike previous hyperbranched PbSe nanowires,[28] no intentional catalyst has been added to break the isotropic crystal growth of PbS and PbSe, leading us to investigate the mechanism responsible for this growth. A clue was suggested in PbSe experiments where the Se boat was inserted 5 cm further into the furnace to higher temperatures and 30 mg of $PbCl_2$ was used. As shown in Figure 4a, these reactions yielded micrometer-sized faceted rods with spherical caps on the tips. EDS line scans along such rods (Figure 4b) reveal that the round balls at the tips to be lead and the microrods to be PbSe. Examination of the binary phase diagrams for Pb−Se (or Pb−S; see Figure S2 in Supporting Information) show that PbSe (or PbS) is the only compound phase in their respective systems and PbSe (or PbS) forms pseudobinary eutectics with Pb. Particularly, Pb metal has a low melting point of 328 °C and can reasonably serve as a VLS catalyst[30,31] for the growth of PbSe (or PbS) nanowires. Even though the observation in Figure 4 is with micrometer-sized rod growth, it does strongly suggest that lead can play the role of VLS catalyst in the formation of nanowires but could be consumed, evaporated, or diffused away[32] during nanowire growth in our experiments. It is likely that the Pb is generated in situ during the CVD growth by reduction from $PbCl_2$, most likely by hydrogen. This eliminates the need for intentional metal catalysts with low melting points previously used to grow hyperbranched PbSe nanowires.[28] Similarly to previously reported metal-catalyzed PbSe nanowires,[28] tapering of the nanowire tip and a length limit to the nanowires of a few tens of micrometers were also observed in our experiments, providing additional circumstantial evidence for this catalyst mechanism. As lead is consumed, the nanowire tapers, and once the lead is consumed, there is no more nanowire growth, limiting the length of the nanowire.

This in situ catalyst formation mechanism could also explain the hyperbranching of PbS and PbSe nanowires. Hydrogen that remains in the CVD system after the initial

bolus can continue to reduce $PbCl_2$, which would continually produce VLS catalysts along the length of the existing nanowire, as shown schematically in Figure 4c. In this sense, the branching growth displayed here is an in situ version of previously demonstrated branched nanowire growth using intentionally added VLS metal catalysts with other materials systems[7,8,33,34] and is most closely related to InAs nanowire formation with continuous feeding of a Mn catalyst.[9] The key difference from previous branching nanowire synthesis is that the VLS catalyst (Pb) is generated continuously in situ, and elemental Pb itself serves as the self-catalyst for the hyperbranched PbQ nanowire growth. It might be possible that hydrogen gas flow can play a similar role for nanowire growth of many other materials[6] for which low melting point metals of the binary system can "self-catalyze" the nanowire growth. However, there is another possibility that hydrogen induces the formation of defects that might promote additional nanowire formation. Defects have previously been suggested as the "active sites" for the growth of straight PbS nanowires.[26] We also note that the solution synthesis of PbSe nanowires can have branches without apparent additional catalysts.[25]

In addition to hydrogen, the surface of the silicon substrates employed has also been found to have a significant effect on the PbS/PbSe CVD deposition and nanostructure growth. All of the results discussed so far were carried out with silicon substrates that are covered with 100 nm of thermal oxide. However, early attempts to synthesize nanowires using a hydrogen-terminated (freshly HF etched) silicon substrate resulted in thick deposition of PbS/PbSe films while growth on silicon substrates with a native oxide reduced the amount of film and cube growth, but not to the desired extent. Unwanted thin film deposition can be kept to a minimum, thus increasing the occurrence of nanowire formation, by using a silicon (100) substrate coated with 100 nm of thermal oxide. It appears that PbS/PbSe preferentially adheres to a fresh silicon surface over oxidized surface. Such surface preference is routinely observed in all successful nanowire synthesis for which a film of PbS/PbSe as thick as 200 μm is always found on the side-exposed silicon edges of freshly cleaved silicon substrates that are otherwise coated with 100 nm oxide.

Raman spectroscopy was collected using a HORIBA Jobin Yvon LabRAM ARAMIS confocal Raman microscope at room temperature with either a 50 mW YAG laser at 532 nm or a 5.5 mW HeNe laser at 632 mW on PbS nanowire clusters or bulk PbS powder (Sigma-Aldrich, 99.9%). Raman spectroscopy can be a useful tool to investigate multiexciton materials as a probe of the exciton−phonon coupling through the Fröhlich interaction. However, PbS is a very weak Raman emitter and should have low wavenumber peaks at 154, 205, and 454 cm^{-1}.[35−37] Attempting to apply intense, energetic laser excitation to produce a significant Raman signal readily led to photo-oxidation of PbS. There are several literature reports of PbS Raman that have photo-oxidation products erroneously assigned as PbS as has been discussed elsewhere.[35]

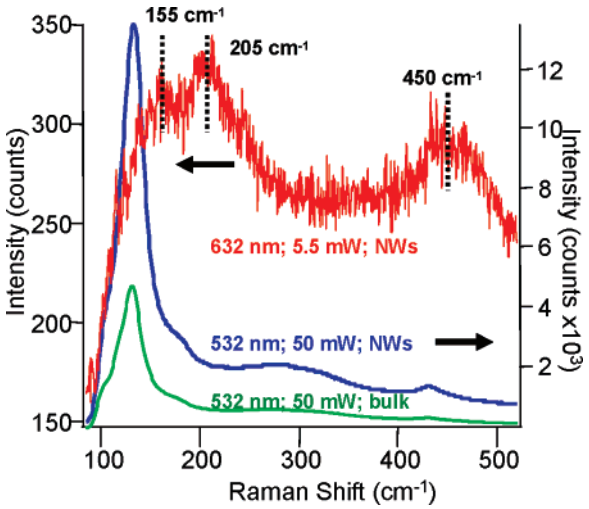

Figure 5. Raman scans of PbS at different laser wavelengths and intensities. The less energetic, less intense 632 nm scan reflects the true PbS spectroscopic response, while the 532 nm spectra of PbS nanowires (NWs) and bulk powder show only photo-oxidation products. The arbitrary scale for the intensity of the bulk PbS spectrum is not shown.

Figure 5 shows the Raman spectra taken on PbS nanowire clusters as well as bulk PbS powder and illustrates the problem of photo-oxidation. Spectra of both PbS reference powder and a PbS nanowire cluster taken at 532 nm showed only one set of peaks independently of laser intensity but shown here most clearly using a 50 mW laser beam. The dominant peak is a 135 cm^{-1} feature that can be assigned to a Pb−O−Pb stretch, while other features at 270 and 429 cm^{-1} can be assigned to $PbO{\cdot}PbSO_4$.[37,38] Interestingly, using a less energetic and less intense laser excitation (632 nm HeNe at 5.5 mW) results in no photo-oxidation, and all three spectral features (upper trace in Figure 5) can be identified as the three commonly reported PbS peaks: 154, 205, and 454 cm^{-1}. Despite an extended collection time of 180 s for the 632 nm spectra from the 5 s for the 532 nm scans, the signal is still 2 orders of magnitude lower than 532 nm spectra. This also suggests that the 632 nm spectrum is due to a weak Raman emitter and not a strong Raman emitter such as Pb−O−Pb. Raman spectra were taken on PbSe nanowire ensembles as well (see Figure S3, Supporting Information) for which photo-oxidation is also likely to be a significant problem that cannot be sorted due to even more limited previous Raman investigations. For further investigation of PbS/PbSe nanomaterials using Raman spectroscopy, great attention must be given to the intensity and wavelength of excitation to ensure the exclusion of photo-oxidation and to allow meaningful Raman investigation of these important materials.

In conclusion, we have reported the CVD synthesis of single-crystalline hyperbranched nanowires of both PbS and PbSe. These nanowires grow along the ⟨001⟩ directions and have a hyperbranched morphology due to a successive secondary growth of nanowires epitaxially from the primary nanowires. The hydrogen gas co-flow is found to greatly influence the morphology from hyperbranched nanowires to simple cubes. It is suggested that in situ generated elemental

Pb due to reduction by hygrogen from the vapor serve as a self-catalyst to nanowire growth and result in the hyperbranched morphology. The Raman spectroscopy of the nanowires was investigated, illustrating the importance of the exclusion of photo-oxidation for Raman investigation of these materials. These nanostructures can find applications in multiple exciton generating photovoltaics, nanospintronics, and in IR detection.

Acknowledgment. This work is supported by a NSF CAREER grant (DMR-0548232). S.J. thanks the 3M Nontenured Faculty Award and the DuPont Young Professor Grant for support. We thank Dr. Alex Kvit for the assistance using the confocal Raman microscope, which is supported by the UW−Madison Materials Research and Engineering Center (MRSEC) (NSF DMR-0520527). We also thank Prof. John C. Wright for helpful discussion on Raman spectroscopy.

Supporting Information Available: EDS of PbSe nanowires, phase diagrams for Pb−S and Pb−Se, and Raman spectroscopy taken on PbSe nanowires and single crystal. This material is available free of charge via the Internet at http://pubs.acs.org.

References

(1) Schaller, R. D.; Klimov, V. I. *Phys. Rev. Lett.* **2004**, *92*, 186601-1.
(2) Ellingson, R. J.; Beard, M. C.; Johnson, J. C.; Yu, P.; Micic, O. I.; Nozik, A. J.; Shabaev, A.; Efros, A. L. *Nano Lett.* **2005**, *5*, 865−871.
(3) Klimov, V. I. *J. Phys. Chem. B* **2006**, *110*, 16827−16845.
(4) Shockley, W.; Queisser, H. J. *J. Appl. Phys.* **1961**, *32*, 510−519.
(5) Qi, D.; Fischbein, M.; Drndic, M.; Selmic, S. *Appl. Phys. Lett.* **2005**, *86*, 093103.
(6) Xia, Y.; Yang, P.; Sun, Y.; Wu, Y.; Mayers, B.; Gates, B.; Yin, Y.; Kim, F.; Yan, H. *Adv. Mater.* **2003**, *15*, 353−389.
(7) Wang, D.; Qian, F.; Yang, C.; Zhong, Z.; Lieber, C. M. *Nano Lett.* **2004**, *4*, 871−874.
(8) Dick, K. A.; Deppert, K.; Larsson, M. W.; Martensson, T.; Seifert, W.; Wallenberg, L. R.; Samuelson, L. *Nat. Mater.* **2004**, *3*, 380−384.
(9) May, S. J.; Zheng, J.-G.; Wessels, B. W.; Lauhon, L. J. *Adv. Mater.* **2005**, *17*, 598−602.
(10) Gudiksen, M. S.; Lauhon, L. J.; Wang, J.; Smith, D. C.; Lieber, C. M. *Nature* **2002**, *415*, 617−620.
(11) Bjork, M. T.; Ohlsson, B. J.; Sass, T.; Persson, A. I.; Thelander, C.; Magnusson, M. H.; Deppert, K.; Wallenberg, L. R.; Samuelson, L. *Appl. Phys. Lett.* **2002**, *80*, 1058.
(12) Wu, Y.; Fan, R.; Yang, P. *Nano Lett.* **2002**, *2*, 83−86.
(13) Lauhon, L. J.; Gudlksen, M. S.; Wang, D.; Lieber, C. M. *Nature* **2002**, *420*, 57−61.
(14) Wachter, P. In *Handbook on the Physics and Chemistry of Rare Earths*; Gschneider, K. A., Jr., Eyring, L., Eds.; North-Holland: Amsterdam, 1979; Vol. 2, pp 507−574.
(15) Krenn, H.; Herbst, W.; Pascher, H.; Ueta, Y.; Springholz, G.; Bauer, G. *Phys. Rev. B* **1999**, *60*, 8117−8128.
(16) Bindilatti, V.; ter Haar, E.; Oliveira, N. F., Jr.; Liu, M. T.; Shapira, Y.; Gratens, X.; Charar, S.; Isber, S.; Masri, P.; Averous, M.; Golacki, Z.; McNiff, E. J., Jr. *Phys. Rev. B* **1998**, *57*, 7854−7862.
(17) Isber, S.; Charar, S.; Fau, C.; Mathet, V.; Averous, M.; Golacki, Z. *Phys. Rev. B* **1995**, *52*, 1678−1682.
(18) Bierman, M. J.; Van Heuvelen, K. M.; Schmeisser, D.; Brunold, T. C.; Jin, S. *Adv. Mater.* **2007**, in press.
(19) Kulkarni, J. S.; Kazakova, O.; Holmes, J. D. *Appl. Phys. A: Mater. Sci. Process.* **2006**, *85*, 277−286.
(20) Wolf, S. A.; Awschalom, D. D.; Buhrman, R. A.; Daughton, J. M.; Von Molnar, S.; Roukes, M. L.; Chtchelkanova, A. Y.; Treger, D. M. *Science* **2001**, *294*, 1488−1495.
(21) Zutic, I.; Fabian, J.; Das Sarma, S. *Rev. Mod. Phys.* **2004**, *76*, 323−410.
(22) Nenadovic, M. T.; Comor, M. I.; Vasic, V.; Micic, O. I. *J. Phys. Chem.* **1990**, *94*, 6390.
(23) Cho, K.-S.; Talapin, D. V.; Gaschler, W.; Murray, C. B. *J. Am. Chem. Soc.* **2005**, *127*, 7140−7147.
(24) Yong, K.-T.; Sahoo, Y.; Choudhury, K. R.; Swihart, M. T.; Minter, J. R.; Prasad, P. N. *Chem. Mater.* **2006**, *18*, 5965−5972.
(25) Hull, K. L.; Grebinski, J. W.; Kosel, T. H.; Kuno, M. *Chem. Mater.* **2005**, *17*, 4416−4425.
(26) Ge, J.-P.; Wang, J.; Zhang, H.-X.; Wang, X.; Peng, Q.; Li, Y.-D. *Chem.—Eur. J.* **2005**, *11*, 1889−1894.
(27) Afzaal, M.; O'Brien, P. *J. Mater. Chem.* **2006**, *16*, 1113−1115.
(28) Zhu, J.; Peng, H.; Chan, C. K.; Jarausch, K.; Zhang, X. F.; Cui, Y. *Nano Lett.* **2007**, *7*, 1095−1099.
(29) Schmitt, A. L.; Bierman, M. J.; Schmeisser, D.; Himpsel, F. J.; Jin, S. *Nano Lett.* **2006**, *6*, 1617−1621.
(30) Wagner, R. S.; Ellis, W. C. *Appl. Phys. Lett.* **1964**, *4*, 89−90.
(31) Morales, A. M.; Lieber, C. M. *Science* **1998**, *279*, 208−211.
(32) Hannon, J. B.; Kodambaka, S.; Ross, F. M.; Tromp, R. M. *Nature* **2006**, *440*, 69−71.
(33) Wan, Q.; Dattoli, E. N.; Fung, W. Y.; Guo, W.; Chen, Y.; Pan, X.; Lu, W. *Nano Lett.* **2006**, *6*, 2909−2915.
(34) Yang, R.; Chueh, Y.-L.; Morber, J. R.; Snyder, R.; Chou, L.-J.; Wang, Z. L. *Nano Lett.* **2007**, *7*, 269−275.
(35) Smith, G. D.; Firth, S.; Clark, R. J. H.; Cardona, M. *J. Appl. Phys.* **2002**, *92*, 4375−4380.
(36) Krauss, T. D.; Wise, F. W. *Phys. Rev. B* **1997**, *55*, 9860.
(37) De Giudici, G.; Ricci, P.; Lattanzi, P.; Anedda, A. *Am. Mineral.* **2007**, *92*, 518−524.
(38) Shapter, J. G.; Brooker, M. H.; Skinner, W. M. *Int. J. Miner. Process.* **2000**, *60*, 199−211.

NL071405L